Synthesis and Evaluation of Alginate-Based Nanogels as Sustained Drug Carriers for Caffeine

Published as part of the ACS Omega virtual special issue "Phytochemistry".

Muhammad Suhail,[&] Chih-Wun Fang,[&] I-Hui Chiu, Arshad Khan, Yi-Chun Wu, I-Ling Lin, Ming-Jun Tsai,* and Pao-Chu Wu*

ACCESS | Metrics & More | Article Recommendations

ABSTRACT: The objective of this study is to design a polymeric network of nanogels for sustained release of caffeine. Therefore, alginate-based nanogels were fabricated by a free-radical polymerization technique for the sustained delivery of caffeine. Polymer alginate was crosslinked with monomer 2-acrylamido-2-methylpropanesulfonic acid by crosslinker N',N'-methylene bisacrylamide. The prepared nanogels were subjected to sol−gel fraction, polymer volume fraction, swelling, drug loading, and drug release studies. A high gel fraction was seen with the increasing feed ratio of polymer, monomer, and crosslinker. Greater swelling and drug release were observed at pH 4.6 and 7.4 as compared to pH 1.2 due to the deprotonation and protonation of functional groups of alginate and 2-acrylamido-2-methyl-propanesulfonic acid. An increase was observed in swelling, loading, and release of the drug with the incorporation of a high feed ratio of polymer and monomer, while a reduction was seen with the increase in crosslinker feed ratio. Similarly, an HET-CAM test was used to evaluate the safety of the prepared nanogels, which showed that the prepared nanogels have no toxic effect on the chorioallantoic membrane of fertilized chicken eggs. Similarly, different characterizations techniques such as FTIR, DSC, SEM, and particle size analysis were carried out to determine the development, thermal stability, surface morphology, and particle size of the synthesized nanogels, respectively. Thus, we can conclude that the prepared nanogels can be used as a suitable agent for the sustained release of caffeine.

1. INTRODUCTION

Caffeine (CFN) (1,3,7-trimethylxanthine) is an alkaloid. It belongs to the family of methylxanthine and is naturally found in coffees, chocolate products, teas, and sodas. It is consumed widely due to its stimulating effect on the central nervous system, which temporarily diminishes drowsiness. Furthermore, CFN acts upon the cardiovascular and respiratory systems and is considered a cause of risk for patients suffering from cardiovascular disorders. In addition, CFN can also cause depression and hyperactivity and exhaust the effects of certain painkillers.[1−3] Caffeine is a highly soluble and highly permeable drug that can be classified as BCS class I. The absorption of CFN occurs very quickly in the small intestine after oral administration at an absorption rate constant (K_{01}) around 0.33 min^{-1}, and the time to reach the maximum plasma concentration varies between 15 min and 2 h because of the delay in gastric emptying and intra-individual difference. CFN is distributed all over the body fluids, tissues, and fetus after absorption. The volume of distribution of CFN ranges between 0.5 and 0.75 L/kg, and it does not accumulate in any specific tissue. About 30 to 75 min (t_{max}) is taken by CFN doses of 5−

8 mg/kg to reach the maximum plasma concentration (C_{max}) level, and it is equal to 8 to 10 mg/L. Normally, a CFN dose of 0.4−2.5 mg/kg is yielded by a cup of black coffee that gives a peak of plasma concentration ranging from 0.25 to 2 mg/L. The virtual complete absorption of CFN takes 45 min in the small intestine after oral consumption to reach 99% bioavailability with no significant first-pass effect.[4] Its bioavailability is also very high, and it crosses the lipid membranes very rapidly. The peak plasma concentration is achieved after oral intake within 15−120 min,[5] while the half-life is within 3−5 h because of its rapid distribution and elimination rate. This demonstrates the recurrent intake of CFN all day to maintain the sufficient blood concentration.[6]

Therefore, a controlled/sustained drug release system is needed, which not only decreases the dose administration frequency and retains the sufficient drug therapeutic level but also enhances the patient compliance. A sustained drug delivery system will be a better option to maintain a patient therapy successfully with a steady increase in the blood level without any burst effect. Therefore, different scientists have worked on the sustained release of caffeine and prepared various carrier systems for sustained delivery of caffeine. Amiri and co-workers prepared caffeine-loaded magnetic alginate beads and reported the sustained delivery of caffeine for 9−9.5 h.[7] Quintanilla de Stéfano et al. developed starch-based hydrogels for the controlled delivery of caffeine up to 13 h.[8] Similarly, Alam and co-workers synthesized caffeine-loaded silica nanoparticle crosslinked thermosensitive hybrid hydrogels for the controlled release of caffeine for 6 h.[9] On the other hand, the authors fabricated polymeric nanogels of alginic acid and reported dynamic swelling and sustained release of caffeine for 24 h.

Although a great development has been made in the delivery of therapeutic agents, still, challenges are needed to be solved, which demand special attention to formulating novel technologies like "nanoparticulate drug delivery systems" ranging between 1 and 1000 nm.[10] Nanoparticulate drug delivery systems involve different approaches such as nanospheres,[11] solid lipid nanoparticles,[12] and liposomes,[13] etc. employed for the actual drug release. Different problems like cost, complex manufacturing methods, low loading of drug, uncertainty, prompt absorption and elimination rate, adverse effects, and exposure to organic solvents exist even though the aforementioned systems have been proven to be promising.[14] Nanogels are a submicron particulate system of hydrogel[15,16] that are prepared by both physical and chemical intercrossing of the polymer.[17,18] Nanogels are prepared by the internal crosslinking and polymerization of polymers to maintain the same structural integrity and absorb a high amount of fluids.[19] Due to their diverse properties such as simple preparation method, tunable size, hydrophilicity, biocompatibility, swelling, and sensitivity to stimuli including light, pH, temperature, biological agents, etc., nanogels are considered as the most suitable next-generation drug delivery systems as compared to other systems.[20] Due to the presence of OH, NH_2, COOH, CONH, $CONH_2$, SO_2H, etc., nanogels capture a high quantity of water and biological fluids.[21] The hydration rate of hydrophobic polymers is up to 5 to 10%, while hydrophilic polymers show a hydration rate up to 90%.[22] Nanogels consolidate the benefits of both nanoparticulate systems and hydrogels as they are a combination of nanosized systems.[23,24]

Hydrogels are three-dimensional structures having the capability to retain a large amount of water without losing structural consistency. Alginate, chitosan, and other polysaccharide polymers are excellent materials for the preparation of hydrogels and their micro/nanoparticulate systems, which are used in various drug delivery systems.[16] Alginates are natural polymers that are employed in various health applications because of their structural similarities to the extracellular matrix. The main benefit of these polymers is their ease of gelation in hot conditions. The sol−gel transition features of the alginates are dependent on their hard egg box-like structures, which are formed due to the binding of functional groups of the adjacent polymeric chains. Alginate is used as impressive macromolecules in the biomedical and pharmaceutical fields.[25,26] Alginate is a polysaccharide composed of 1,4-linked β-D-mannuronic acid (M) and α-L-guluronic acid (G) monomers. Stable complexes are formed by the G−G sequences in the presence of divalent cations due to the so-called "egg box junctions". Usually, the quick release of CFN from the prepared polymeric matrix system is the result of the high solubility and poor interaction of CFN with the polymer matrix. Therefore, the authors prepared alginate-based nanogels to sustain the release of CFN for an extended period of time. Alginate has been used in combination with other compounds for the *in vitro* release of CFN.[27] Some examples are Alg/$CaCO_3$ hydrogel colloidosomes,[28] chitosan-coated alginate microhydrogels,[29] and Alg beads combined with pectin, carrageenan, chitosan, and psyllium husk.[30] 2-Acrylamido-2-methylpropanesulfonic acid (AMPS) is a water-soluble monomer that exhibits both an ionic and nonionic nature. Due to its hydrophilic nature, the white crystalline AMPS powder is dissolved very fast in water. The ionized sulfonate functional groups of AMPS are responsible for its swellability. The better stability of AMPS against hydrolysis is because of its ionized sulfonate groups, which dissociate completely in the entire pH range,[31] and thus it shows a strong resistance to salt. AMPS is swelled greatly when it is exposed to a medium with a specific pH.[32,33] AMPS is widely used as superabsorbents, soft-biomimetic actuators, and biomaterials for water purification and in the bioengineering, agriculture, and food industry.[34−36]

The novelty of the synthesized nanogels is based on the incorporation of AMPS with natural polysaccharide polymer alginic acid, which not only prolong the release of CFN but also overcome the encountered side effects of CFN with its rapid administration. As alginic acid is nontoxic in nature, its combination with AMPS led to the development of safe and stable polymeric nanogels, which exhibited maximum swelling, loading, and release of drugs. An HAT-CAM test is a new technique employed for the toxicological evaluation of alginic acid and prepared nanogels, and the results indicated that alginic acid and the developed nanogels have no toxic effects. Similarly, characterizations such as FTIR, DSC, and SEM were conducted, which confirmed the preparation and nature of the prepared nanogels. Thus, we can conclude that the novel prepared nanogels of alginic acid can be considered the most suitable drug carrier system for the sustained delivery of drugs.

2. MATERIALS AND METHODS

2.1. Materials. AMPS and CFN were obtained from Alfa Aesar, Lancashire, U.K. Alginic acid (Al) was procured from Across Organic, Janssen Pharmaceuticalaan, Belgium. Similarly, ammonium persulfate (APS) and N',N'-methylene bisacrylamide (MBA) were purchased from Showa, Tokyo, Japan and Alfa Aesar, Lancashire, U.K., respectively.

2.2. Fabrication of Polymeric Nanogels. The fabrication of alginate-*graft*-poly(2-acrylamido-2-methylpropanesulfonic acid) (Al-*g*-pAMPS) nanogels was carried out via a free-radical polymerization technique. Hence, the solution of Al was formed in 10 mL of deionized distilled water while keeping a constant temperature of 50 °C with 50 rpm. Similarly, AMPS and APS solutions were formed in deionized distilled water separately. APS and AMPS solutions were mixed together, and after proper mixing, the mixture was poured into the Al solution. MBA is not completely soluble in water; hence, a mixture of ethanol and water (1:1 v/v) was employed for dissolving MBA. Finally, MBA solution was added dropwise into a mixture of polymer and monomer. The mixture was kept

on a constant stirring for 18−22 min. The prepared transparent solution was subjected to nitrogen purging to eliminate any dissolved oxygen. After that, the transparent solution was transferred into glass molds, which were placed in a water bath at 70 °C for 6−7 h. The prepared gel was passed through sieve number 20, and fine gel particles were obtained, which were washed by a mixture of water and ethanol. The fine gel particles were placed initially at room temperature for 24 h and then positioned in a vacuum oven at 40 °C for drying. The dried particles of gel were passed through sieve 625 again to obtain nanogel particles. The synthesized nanogels were subjected to a series of studies and characterizations. The different combination ratios of polymer, monomer, and crosslinker are shown in Table 1, while the proposed chemical structure of the prepared nanogels is presented in Figure 1.

Table 1. Feed Ratio Scheme for the Formulation of Al-*g*-pAMPS Nanogels

formulation code	polymer Al (g/100 g)	monomer AMPS (g/100 g)	initiator APS (g/100 g)	crosslinker MBA (g/100 g)
AMF-1	0.32	14	0.2	4
AMF-2	0.52	14	0.2	4
AMF-3	0.72	14	0.2	4
AMF-4	0.32	16	0.2	4
AMF-5	0.32	18	0.2	4
AMF-6	0.32	20	0.2	4
AMF-7	0.32	14	0.2	6
AMF-8	0.32	14	0.2	8
AMF-9	0.32	14	0.2	10

2.3. Characterizations. Characterizations such as FTIR, DSC, SEM, and XRD were performed according to our previous publication.[37] The particle size of the prepared nanogels was determined by dynamic light scattering (DLS) (ELSZ-2000 particle size analyzer, Otsuka Electronics, Otsuka, Japan). Hence, the nanogel particles were dispersed in acetone. A suspension was formed, which was processed further for the particle size analysis.[38]

2.4. Sol−Gel Fraction Analysis. A Soxhlet extraction method was employed for the determination of sol and gel fractions. Hence, a weighed amount of nanogels was subjected to the Soxhlet extraction process. Deionized distilled water was used throughout the experiment. The extraction process was carried out for 12 h at 80 °C. After that, nanogels were collected and dried in a vacuum oven at 40 °C, which were weighed again.[39,40] The following equations were used for the estimation of sol and gel fractions:

$$\text{sol fraction\%} = \frac{C_1 - C_2}{C_1} \times 100 \tag{1}$$

$$\text{gel fraction} = 100 - \text{sol fraction} \tag{2}$$

C_1 indicates the initial weight of the dried nanogels, whereas C_2 represents the final weight after the extraction process.

2.5. *In Vitro* Swelling Studies. The swelling index of the fabricated nanogels was determined in a dialysis membrane at pH 1.2, 4.6, and 7.4. A weighed quantity of nanogels was placed in the dialysis membrane and then immersed in the respective pH medium. The membrane containing the nanogels was removed from the buffer solutions after allowing proper swelling at specific time intervals. The membrane was

blotted with the help of a filter paper, weighed, and immersed back in the respective buffer solution. This action was repeated until a constant weight of the swelled nanogels was achieved.[41] The swelling ratio was determined by using the following equation:

$$q = \frac{A_2}{A_1} \tag{3}$$

q represents the dynamic swelling, A_1 indicates the initial weight of the dried nanogels before swelling, and A_2 represents the final weight after swelling at time t.

2.6. Polymer Volume Fraction. The fraction of polymer in swelled state was determined for the developed nanogels in three media with various pH, i.e., pH 1.2, 4.6, and 7.4. It is represented by V2,s. The polymer volume fraction was determined by employing equilibrium volume swelling (Veq) data.[42] The following equation was used for the estimation of polymer volume fraction:

$$\text{V2, s} = \frac{1}{\text{Veq}} \tag{4}$$

2.7. Drug Loading. An absorption and diffusion method was adopted for loading of CFN to the developed nanogels. Nanogels of accurate weight were placed in 1% CFN solution of phosphate buffer. After that, nanogels were immersed for 24 h at 25 °C, and then lyophilization of nanogels was carried out to eliminate any entrapped solvent.[43]

The amount of drug loaded by the prepared nanogels was determined by an extraction method. Loaded particles of nanogels of accurate weight were submerged in 100 mL phosphate buffer solution of pH 7.4. The suspension was kept stirring until all the loaded drug was removed completely from the nanogel particles. After that, a filter membrane was used for the filtration of suspension that was then analyzed on a UV−vis spectrophotometer (U-5100, 3J2-0014, Tokyo, Japan) at λ_{max} 230 nm in triplicate.[44]

2.8. HET-CAM Test. The anti-irritant properties, anti-inflammatory potential, and toxicity/ocular toxicity of the materials were evaluated through the HET-CAM test by a number of scientists.[45] Thus, in the current investigation, the authors performed the HET-CAM test for the Al and developed nanogels to determine their toxic effects. Therefore, 300 μL samples of Al and prepared nanogels were applied on the chorioallantoic membrane of fertilized chicken eggs at regular time intervals. Various parameters like coagulation, hemorrhage, and vasoconstriction were detected during the experiment. 1% Sodium lauryl sulfate and 0.9% NaCl were used as positive and negative controls, respectively.[46] The irritation index was determined by taking the sum of the scores of each injury as shown in the following equation:

$$\text{irritation index} = \frac{(301 - H) \times 5}{300} + \frac{(301 - V) \times 7}{300}$$
$$+ \frac{(301 - C) \times 9}{300} \tag{5}$$

where H, V, and C indicate the hemorrhage, vasoconstriction, and coagulation at time (s).

2.9. *In Vitro* Drug Release Studies. *In vitro* release studies of CFN from the developed nanogels were conducted in the same pH values as swelling studies, i.e., pH 1.2, 4.6, and 7.4. A Dissolution apparatus type II (Sr8plus Dissolution Test Station, Hanson Research, Chatsworth, CA, USA) was used for
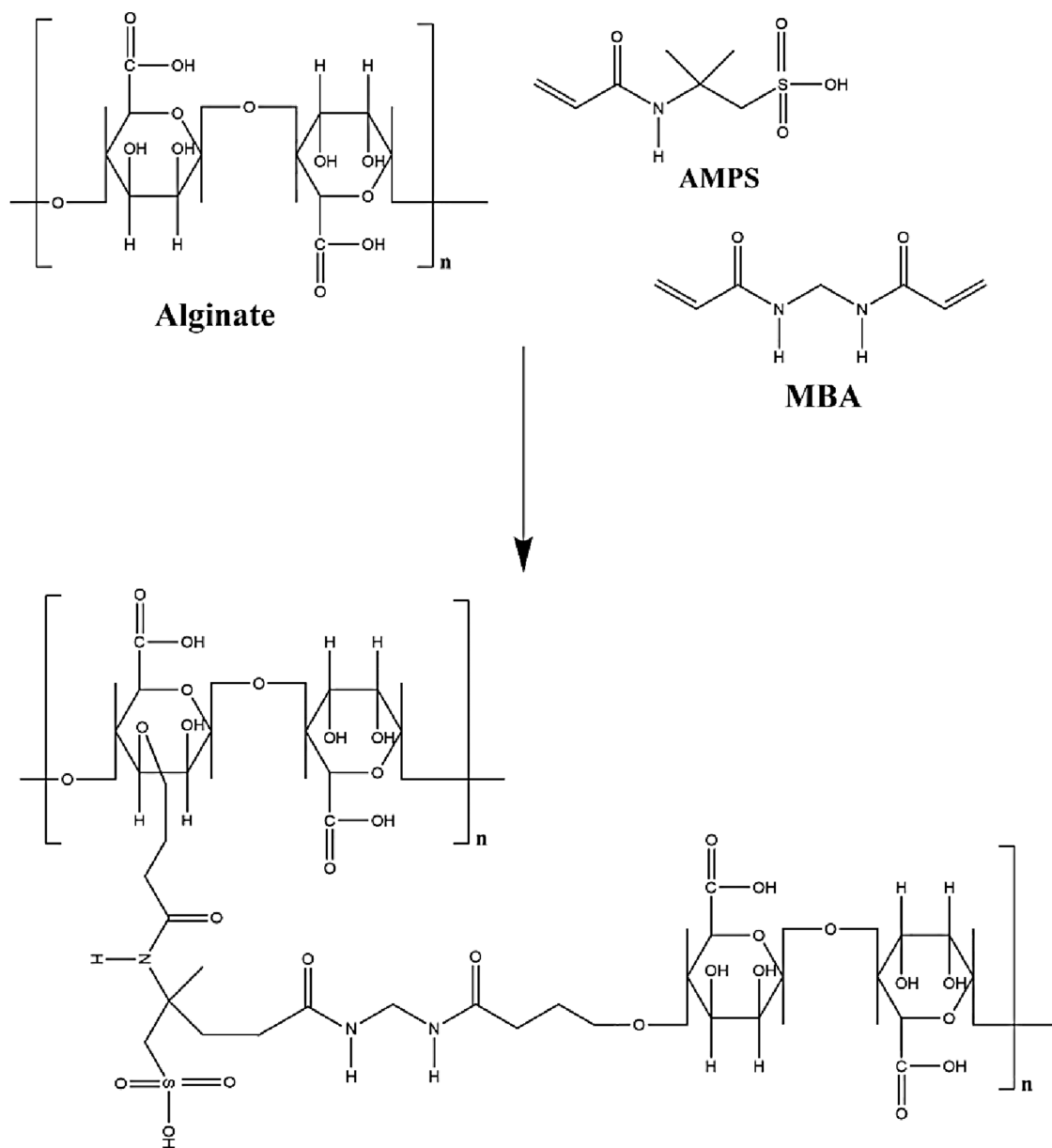
Figure 1. Proposed chemical structure of Al-*g*-pAMPS nanogels.

drug release studies. A 500 mL respective buffer solution was placed in the dissolution apparatus. A weighed nanogel containing the drug was placed in dialysis membranes, which were submerged in the buffer solution at 37 ± 0.5 °C and 50 rpm. To maintain the sink condition throughout the investigation, a 5 mL sample of the medium was taken at regular intervals, and a new medium with the same concentration was added back. The samples were then examined using a UV−Vis spectrophotometer (U-5100, 3J2-0014, Tokyo, Japan) in triplicate at a maximum wavelength of 230 nm.[47]

Different kinetic models including zero-order kinetics, first-order kinetics, Higuchi model, and Korsmeyer−Peppas model were used for the prepared nanogels. Thus, interpretation of the drug release data was carried out to evaluate both the order and mechanism of drug release.[48]

2.10. Statistical Analysis. Statistical analysis of all investigations was done using SPSS Statistic 22.0 (IBM Corp, Armonk, NY, US). The Student's *t*-test was used to determine whether there were any differences between the tests. The results were considered significant when the *p*-value was less than 0.05.

3. RESULTS AND DISCUSSION

3.1. Fabrication of Polymeric Nanogels. Al-*g*-pAMPS nanogels were prepared by the crosslinking and polymerization of Al with AMPS in the presence of APS and MBA. The different combinations of Al, AMPS, and MBA affected the various parameters of the prepared nanogels. With the increasing concentration of MBA, a hard network of nanogels was formed, which delayed the motility of the nanogel networks. As a result, the swelling, loading, and release of the drug were reduced. On the other hand, nanogel networks with high concentrations of Al and AMPS exhibited an increase in the aforementioned parameters due to the increase in motility and vice versa. The physical appearances of the prepared nanogels with high concentrations of MBA, Al, and AMPS are shown in Figure 2.

Figure 2. Physical appearances of Al-*g*-pAMPS nanogels with high incorporated concentrations of (A) MBA, (B) Al, and (C) AMPS.

3.2. FTIR. FTIR is used to evaluate the functional groups of reagents and formulations. The FTIR spectra of Al, AMPS, CFN, and the unloaded and the drug-loaded nanogels are shown in Figure 3. The FTIR spectrum of Al indicated a broad
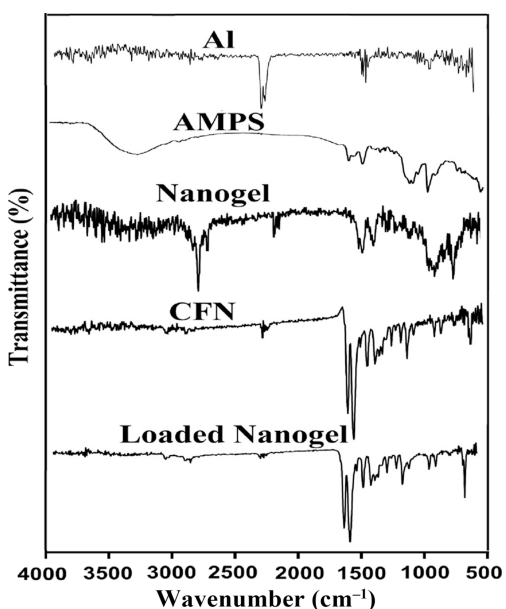
Figure 3. FTIR spectra of Al, AMPS, nanogels, CFN, and drug-loaded nanogels.

centered peak at 3410 cm^{-1} assigned to the O−H stretching vibration, while the peak at 2932 cm^{-1} presented the stretching vibration of C−H. The existence of the asymmetric stretching vibration of carboxylate O−C−O was verified by the band at 1608 cm^{-1}. Similarly, a peak at 1420 cm^{-1} may be correlated to the deformation of C−OH with the symmetric vibration of the carboxylate O−C−O group. A weak peak at 1040 cm^{-1} may be related to the stretching vibration of C−O and C−C of pyranose rings. The same peaks of Al were reported by Sivagnanavelmurugan and co-workers, which further supports our findings.[49] The FTIR spectra of AMPS revealed structural peaks at 1658 and 1559 cm^{-1}, indicating the C=O stretching (amide I band) and N−H bending (amide II band). Two characteristics peaks at 1240 and 1370 cm^{-1} confirmed the existence of the SO$_3$H group, indicating the symmetrical and asymmetrical stretching vibrations of the S=O group. The C−H stretching vibration was depicted by a peak at 2990 cm^{-1}. A prominent absorption peak within the 828−1080 cm^{-1} range indicated the S-O-C group.[50] Due to the polymerization reaction among nanogel contents, certain peaks of Al and AMPS were modified in the developed networks of nanogels.

The distinct peaks of Al and AMPS at 1608, 2932, and 1370, 1559 cm^{-1} shifted to 1630, 2890, 1405, and 1575 cm^{-1} for the synthesized nanogels. Some new peaks were formed, while a few disappeared. These all indicated the development of a new polymeric nanogel network. Similarly, the FTIR spectra of CFN exhibited a characteristic peak at 3412 cm^{-1}, which is assigned to the stretching vibration of N−H. Similarly, peaks at 2948 and 3110 cm^{-1} indicated the aromatic stretching of C−H. A band at 1658 cm^{-1} represented the −C=N ring stretching.[51,52] Modification was seen in certain peaks of the prepared nanogels after being loaded with CFN. Peaks at 1658 and 2948 cm^{-1} were shifted slightly to 1670 and 2935 cm^{-1} for the loaded nanogels. The presence of drug peaks in the loaded nanogels indicated the successful loading of CFN without any kind of interaction with the nanogel reagents.[53]

3.3. DSC. The thermal stability of the unreacted Al, AMPS, and prepared nanogels was investigated by DSC (Figure 4).
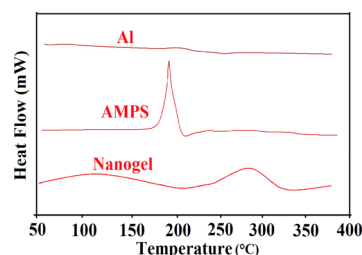
Figure 4. DSC of Al, AMPS, and Al-*g*-pAMPS nanogels.

The DSC thermogram of Al exhibited two endothermic peaks at 60 and 250 °C, whereas two exothermic peaks at 202 and 348 °C were detected, respectively. Endothermic peaks indicated the water elimination of the hydrophilic groups.[54] Similarly, the DSC thermogram of AMPS presented an exothermic peak at 199 °C, whereas an endothermic peak was perceived at 210 °C, representing the glass transition temperature. The AMPS degradation was observed through an exothermic peak at 199 °C.[55] Likewise, the DSC thermogram of the developed nanogels exhibited two exothermic peaks at 248 and 280 °C, while two endothermic peaks were depicted at 200 and 330 °C, respectively. The DSC thermogram of the synthesized nanogels demonstrates an alteration in the endothermic and exothermic peaks of the Al and AMPS. The exothermic and endothermic peaks of the Alg and AMPS at 202, 199 °C and 250, 210 °C shifted to 248, 280 °C and 200, 330 °C for the prepared nanogels. Due to crosslinking of Al with AMPS in the presence of APS and MBA, the exothermic and endothermic peaks of both Al and AMPS were modified, as shown by the DSC thermogram of the synthesized nanogels, which confirmed the preparation of a highly stable and polymeric network of nanogels, and thus an increase in the thermal stability of reagents was observed, as shown by the DSC thermogram of synthesized nanogels. Barkat and co-workers synthesized hydrogels of chondroitin sulfate and presented an increase in the thermal stability of the reagent after polymerization.[56]

3.4. Scanning Electron Microscopy (SEM) and Particle Size Analysis. The surface morphology of the fabricated nanogels has a key role in swelling and drug loading. SEM is employed to analyze the surface nature of the fabricated system. The surface of the prepared nanogels was found to be very dense with a few pores, as indicated in Figure 5. The dense surface may be correlated with the high crosslinking
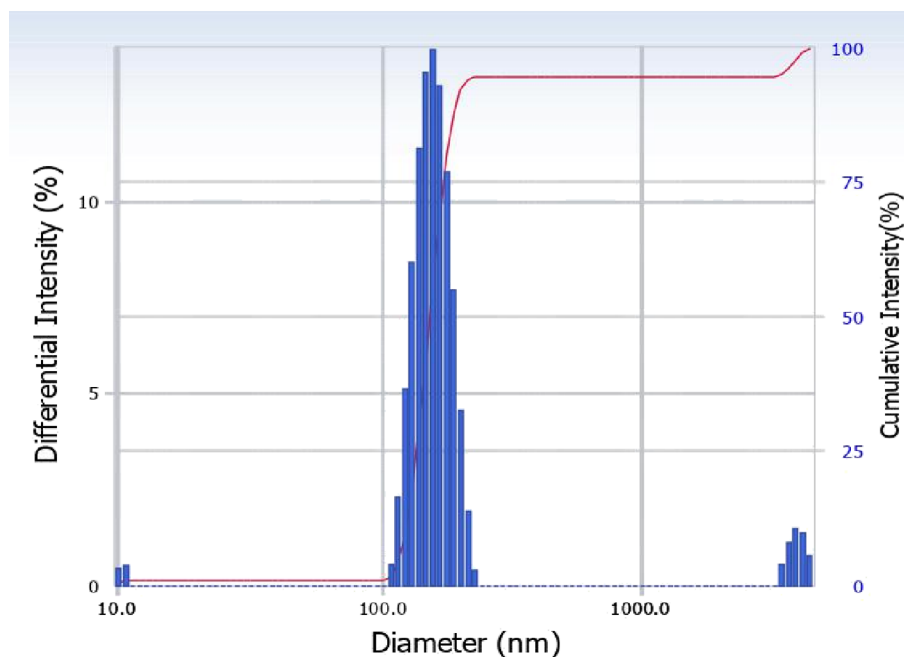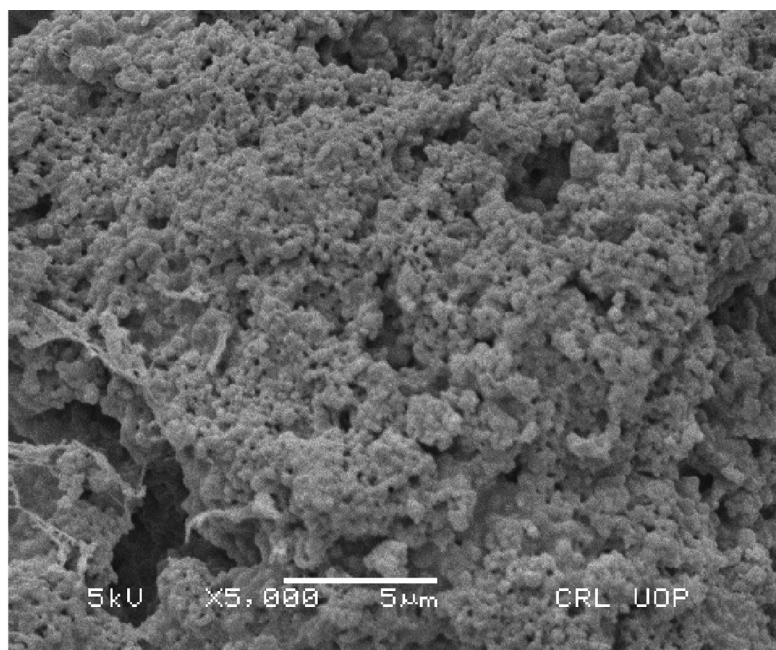
Figure 5. SEM and particle size of Al-*g*-pAMPS nanogels.

among nanogel contents.[57] Particle size plays a crucial role in swelling, loading, and release of the drug. Dynamic light scattering (DLS) was used for particle size determination of the developed nanogels. The prepared nanogels exhibited an average particle of 408 nm with a polydispersity index of 0.100.[58,59] The amount of reagents consumed in the synthesis of a system influenced the particle size of the formulated system. The small particle size leads to the large surface of the nanogels, and thus high swelling, loading, and drug release will be achieved.

3.5. Sol−Gel Fraction Analysis. The sol−gel fraction was determined for all nanogel formulations, as shown in Figure 6. Sol is the uncrosslinked soluble fraction, while gel is the crosslinked insoluble fraction of the prepared nanogels. Nanogel contents have highly influenced both sol and gel

fractions. As the Al and AMPS feed ratios were increased, an increase in the gel fraction was seen. Free radicals are generated during the polymerization, which are responsible for crosslinking and polymerization among nanogel contents. With an increase in the feed ratios of polymer and monomer, an increase in generation of free radicals was detected. Hence, the higher the concentration of Al and AMPS, the more rapid the generation of free radicals and thus the higher the availability of reactive sites for the gelation process, which leads to a high gel fraction. Similarly, the crosslinking between Al and AMPS was increased with the usage of a high concentration of MBA, which is responsible for the cross-linking of both Al and AMPS on their active sites. So, the greater the concentration of MBA, the faster the polymer-ization between Al and AMPS and the higher the gel
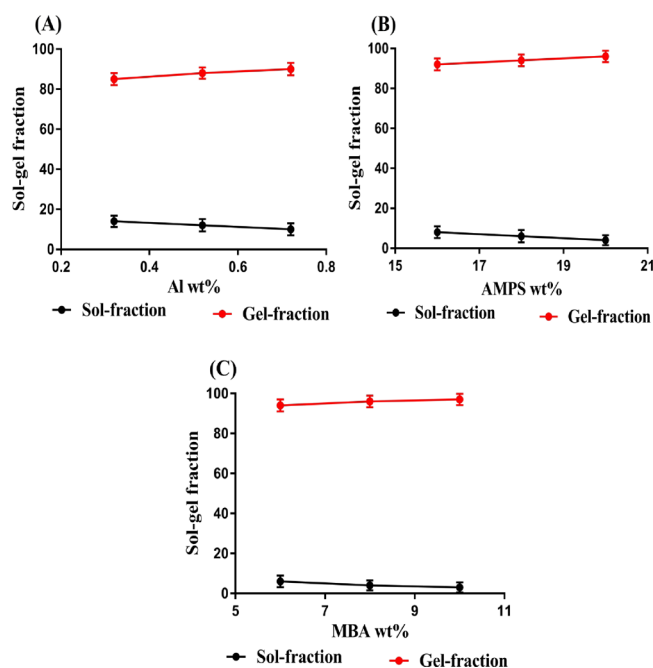
Figure 6. Effect of (A) Al, (B) AMPS, and (C) MBA on the sol−gel fraction.

Figure 7. Effect of (A) pH, (B) Al, (C) AMPS, and (D) MBA on dynamic swelling of Al-*g*-pAMPS nanogels.

fraction.[60,61] Khalid et al. synthesized polymeric hydrogels for controlled drug delivery and demonstrated a high gel fraction of the prepared hydrogels.[62] In contrast to the gel fraction, a reduction in sol fraction was seen as the compositions of Al, AMPS, and MBA increased.[63] Nasir and co-workers developed polymeric gels and demonstrated a high gel fraction with low sol fraction for the prepared gel.[64]

3.6. *In Vitro* Swelling Studies. Swelling studies were performed on the developed nanogels in buffer solutions of pH 1.2, 4.6, and 7.4. pH affected the swelling index of the prepared nanogels as high swelling was observed at pH 4.6 and 7.4 as compared to pH 1.2 (Figure 7A). Al consists of COOH functional groups, while AMPS contains SO$_3$H functional groups. At pH 1.2, the functional groups of the polymer and monomer were protonated, and strong hydrogen bonds allowed them to form conjugates with the counter ions. Due to the formation of conjugates, the overall charge density of nanogels was decreased, and therefore, low swelling was achieved. On the other hand, as the pH of the medium changes, a shift in the nanogels' swelling is also seen. High swelling was shown by the prepared nanogels at pH 4.6 and 7.4. The main reason is the deprotonation of Al and AMPS functional groups, which results in a high charge density, which exhibited strong electrostatic repulsive forces, and thus an increase and expansion in the volume of nanogels occurred. Hence, an increase in swelling of the formulated nanogels was shown at pH 4.6 and especially at pH 7.4.[32,62,65,66]

Like pH, nanogel contents also influenced the swelling index as high swelling was achieved with the high feed ratios of Al and AMPS. The high concentration of Al led to the generation of COOH groups in a high amount. Similarly, an increase in the AMPS concentration led to high density of SO$_3$H groups. Due to the high charge density of COOH and SO$_3$H groups of Al and AMPS, greater repulsive forces were generated, and therefore, high swelling of nanogels was seen (Figure 7B,C).[67−69] Contrary to Al and AMPS, a reduction in the swelling of nanogels was observed with the high incorporation
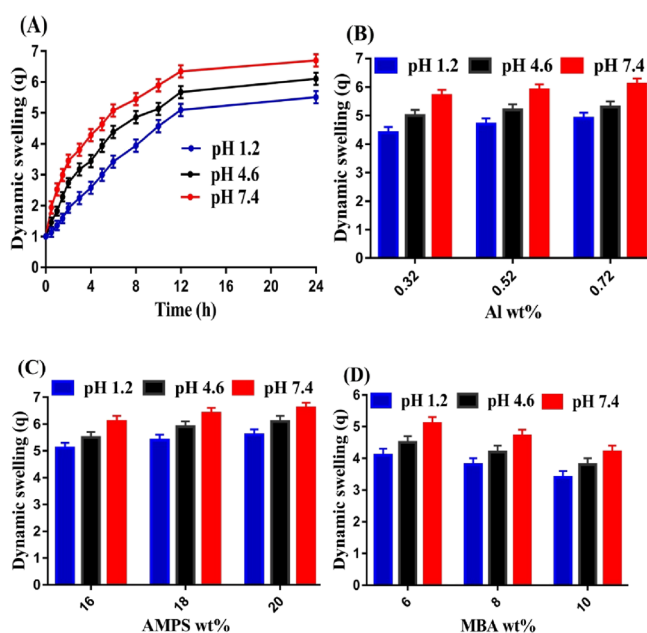
of MBA contents. A hard and tough network of nanogels was formed, which decreased the pore size and motility of the synthesized nanogels. Thus, a decline in swelling was observed with the increasing concentration of MBA (Figure 7D) and vice versa.[70,71]

3.7. Polymer Volume Fraction. The polymer volume fraction indicated the volume of polymer in the swelled state. This study was performed in pH 1.2, 4.6, and 7.4, as shown in Table 2. At pH 1.2, a high polymer volume fraction was

Table 2. Polymer Volume Fraction and Drug Loading of Al-*g*-pAMPS Nanogels

	polymer volume fraction			
F. code	pH 1.2	pH 4.6	pH 7.4	drug loaded (mg)/500 mg of dry gel via an extraction method
AMF-1	0.223	0.198	0.172	133.3 ± 0.2
AMF-2	0.210	0.187	0.166	168.4 ± 0.1
AMF-3	0.204	0.182	0.163	180.1 ± 0.3
AMF-4	0.194	0.178	0.158	194.4 ± 0.4
AMF-5	0.187	0.170	0.151	210.2 ± 0.2
AMF-6	0.181	0.165	0.147	218.6 ± 0.3
AMF-7	0.239	0.220	0.193	126.7 ± 0.2
AMF-8	0.256	0.234	0.212	118.8 ± 0.1
AMF-9	0.289	0.256	0.237	105.7 ± 0.2

achieved as compared to pH 4.6 and 7.4. The reason may be correlated with the swelling index of the nanogel as there is an inverse relationship between the polymer volume and swelling index. An increase and decrease in one content leads to the decrease and increase in the other content. The polymer volume fraction has been affected by nanogel contents since a drop in polymer volume fraction was seen with increased feed ratios of Al and AMPS. On the other hand, as the feed ratio of MBA was increased, an increase in the polymer volume fraction was seen. The high swelling at pH 1.2 and low swelling at pH 4.6 and 7.4 demonstrated the proficient and excellent swelling of the prepared nanogels at pH 4.6 and 7.4 as

compared to pH 1.2. Similarly, the low polymer volume fraction of Al and AMPS and high polymer volume fraction of MBA at pH 1.2, compared to 4.6 and 7.4, demonstrated the potential and high swelling index of the prepared nanogels at pH 4.6 and 7.4 as compared to pH 1.2 with the increasing concentration of Al and AMPS, while a decrease in swelling was observed with the increase in MBA content.[42]

3.8. Drug Loading. The loading of drug was completely dependent on the swelling of the fabricated nanogels.[72] Due to the high swelling index of the nanogels in the phosphate buffer solution of pH 7.4, a maximum loading of drug was achieved, as indicated in Table 2. Drug loading was affected by the different combinations of the nanogel contents. An increase in loading of drug was detected with the increasing feed ratios of Al and AMPS. Unlike the Al and AMPS, the loading of drug was decreased with the incorporation of high MBA contents due to the low swelling degree of the fabricated nanogels. The pore size of the nanogels was decreased with high MBA feed ratios, which retarded the movement of the nanogel networks, and as a result, less penetration of water into the nanogel network occurred. Thus, a reduction in loading of the drug occurred in the end.[72,73]

3.9. *In Vitro* Drug Release Studies. Drug release studies were carried out for the prepared nanogels in three different buffer solutions, i.e., pH 1.2, 4.6, and 7.4. Like swelling, the drug release was also influenced by the pH of the medium as relatively low swelling was achieved at pH 1.2, while maximum drug release was detected at pH 4.6 and especially at pH 7.4, as indicated in Figure 8A. The low release of the drug at pH 1.2
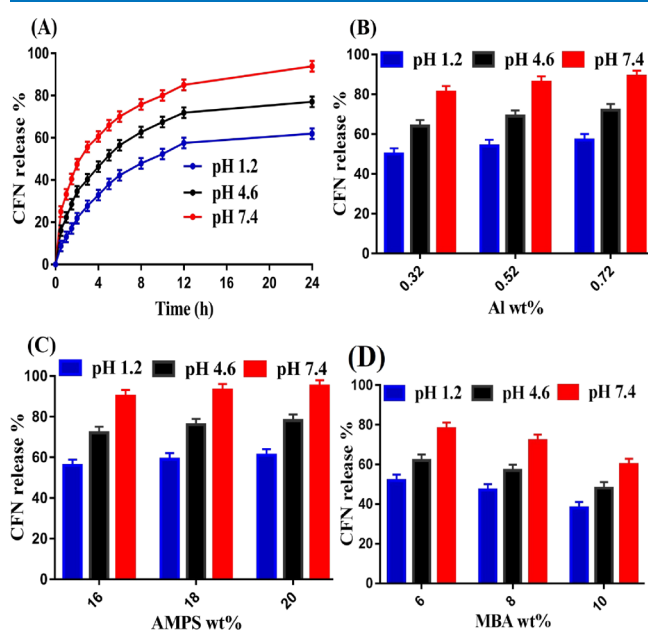
Figure 8. Effect of (A) pH, (B) Al, (C) AMPS, and (D) MBA on the drug release from Al-*g*-pAMPS nanogels.

was due to the protonation of COOH and SO$_3$H groups of the Al and AMPS, which decreased the overall charge density of the nanogel network. Thus, a decline in drug release was perceived. On the other side, the drug release was increased with the change in the pH of the medium from 1.2 to 4.6 and 7.4. The reason may be related with the deprotonation of functional groups of the Al and AMPS, which results in high swelling and release of drug.[32,33,74]

Nanogel contents have also influenced the drug release for the developed nanogels (Figure 8B−D). Drug release was improved as the feed ratios of the Al and AMPS were increased.[67] The charge density of the functional groups of Al and AMPS increased, which results in high swelling and release of drug. Contrary to polymer and monomer contents, as the feed ratio of MBA was increased, a reduction in the drug release was noticed. The reason may be linked with the low swelling of the nanogel, and thus a decrease in drug release was achieved and vice versa.[75] Ali and co-workers prepared hydrogels of polyvinyl alcohol and reported an increase in drug release with the high composition of Al and AMPS, while MBA revealed the opposite effect.[57]

The analysis of linear regression was carried out for the kinetic of CFN from the prepared nanogel. "*r*" values determined the order of the drug release from the fabricated nanogels. The "*r*" values of the Korsmeyer−Peppas model for all formulations of the nanogels were found to be very close to 1 as compared to the "*r*" values of others models. Thus, the Korsmeyer−Peppas model is considered as the best fit and most applicable model of kinetics. Diffusion types for the Korsmeyer−Peppas model include Fickian diffusion ($n \leq 0.45$) and non-Fickian transport ($n > 0.45$).[76] Both the "*r*" and "*n*" values of the developed nanogels are shown in Table 3. The "*n*" values were found within the 0.2575−0.4252 range, indicating Fickian diffusion of the developed nanogels.

Table 3. Kinetic Modeling Release of KT from Al-*g*-pAMPS Nanogels

F. code	zero order r^2	first order r^2	Higuchi r^2	Korsmeyer−Peppas r^2	n
AMF-1	0.6759	0.8702	0.9138	0.9840	0.2875
AMF-2	0.6983	0.9907	0.9848	0.9940	0.2575
AMF-3	0.6273	0.9146	0.9643	0.9819	0.3230
AMF-4	0.8836	0.9895	0.9703	0.9922	0.4069
AMF-5	0.6442	0.8821	0.9553	0.9835	0.4252
AMF-6	0.6673	0.9572	0.9641	0.9707	0.3790
AMF-7	0.7163	0.9185	0.9850	0.9873	0.3147
AMF-8	0.9306	0.9357	0.9905	0.9943	0.2930
AMF-9	0.9092	0.9732	0.9543	0.9932	0.3234

3.10. HET-CAM Test. The toxicological analysis of the Al and prepared nanogels is indicated in Figure 9 and Table 4. The chorioallantoic membrane of the chicken egg was treated with Al and the prepared nanogels at predetermined time intervals, i.e., 0, 0.5, 1, 5, and 30 min. The negative control must show no toxic effect, while the positive control must show toxic effects or vascularization signs of hemorrhage, vasoconstriction, and coagulation phenomena after application. Thus, 1% sodium lauryl sulfate (SLS) was used in the current investigation as a positive control and 0.9% NaCl as a negative control. The irritation index for the negative control was found to be zero (0), while for the positive control, a very high index of irritation was achieved (6.92) after application. Likewise, the irritation index for Al and the prepared nanogels scored 0.02 and 0.01, respectively. Hsieh and co-workers demonstrated the same results as our investigation, which supports further our findings.[77] Finally, we can demonstrate that the prepared nanogel network had no adverse effects and can be used as a promising drug delivery system.
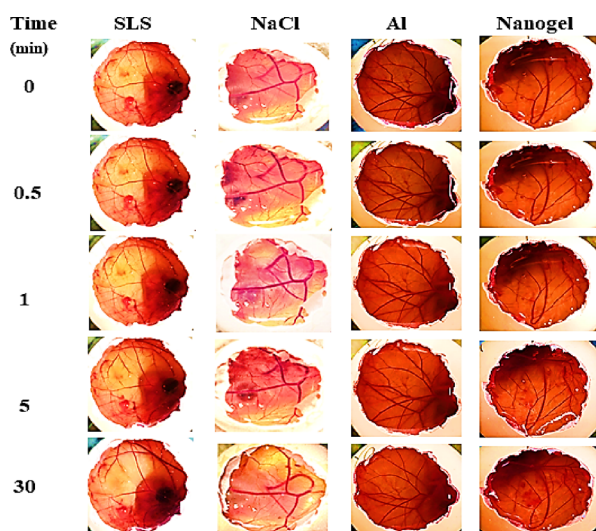
Figure 9. Toxicological evaluation of SLS, NaCl, Al, and Al-*g*-pAMPS nanogels on the chorioallantoic membrane of fertilized chicken eggs.

Table 4. Irritation Indexes of SLS, NaCl, Al, and Prepared Nanogel

formulation	irritation index	classification
SLS	6.92	irritating
NaCl	0.00	non-irritating
Al	0.02	non-irritating
nanogel	0.01	non-irritating

4. CONCLUSIONS

Polymerization among nanogel contents resulted in the prepared nanogels. FTIR proved the preparation and compatibility of the crosslinked nanogels. SEM indicated a dense surface with few pores. An average particle size of 408 nm was found, which is most suitable for high swelling, loading, and release of drug. High swelling and drug release were seen at pH 7.4 and 4.6 as compared to pH 1.2. Crosslinked nanogels exhibited to a low sol fraction with a high gel fraction with the increasing composition of Al, AMPS, and MBA. Drug loading was affected by the various compositions of nanogel contents. A decline was seen in drug loading with high MBA incorporation, while Al and AMPS presented direct effects on drug loading contrary to MBA. Similarly, safety of the prepared nanogels was investigated by the HET-CAM test, which proved the safe use of nanogels for oral administration of CFN. Conclusively, results show that the fabricated nanogels could be considered the most suitable agent for sustained drug delivery systems.

■ AUTHOR INFORMATION

Corresponding Authors

Ming-Jun Tsai − *School of Medicine, College of Medicine, China Medical University, Taichung 404, Taiwan; Department of Neurology, China Medical University Hospital, Taichung 404, Taiwan; Department of Neurology, An-Nan Hospital, China Medical University, Tainan 709, Taiwan*; Phone: +886 4 22052121; Email: 25570@ tool.caaumed.org.tw, d22570@mail.cmuh.org.tw

Pao-Chu Wu − *School of Pharmacy and Drug Development and Value Creation Research Center, Kaohsiung Medical University, Kaohsiung 807, Taiwan; Department of Medical Research, Kaohsiung Medical University Hospital, Kaohsiung 807, Taiwan;* ◉ orcid.org/0000-0001-8852-0534; Phone: +886 7 3121101; Email: pachwu@kmu.edu.tw

Authors

Muhammad Suhail − *School of Pharmacy, Kaohsiung Medical University, Kaohsiung 807, Taiwan*

Chih-Wun Fang − *Division of Pharmacy, Zuoying Branch of Kaohsiung Armed Forces General Hospital, Kaohsiung 813, Taiwan*

I-Hui Chiu − *School of Pharmacy, Kaohsiung Medical University, Kaohsiung 807, Taiwan*

Arshad Khan − *Department of Pharmaceutics, Faculty of Pharmacy, The Islamia University of Bahawalpur, Bahawalpur 63100, Pakistan*

Yi-Chun Wu − *School of Pharmacy, Kaohsiung Medical University, Kaohsiung 807, Taiwan*

I-Ling Lin − *Department of Medicine Laboratory Science and Biotechnology, College of Health Science, Kaohsiung Medical University, Kaohsiung 807, Taiwan; Department of Laboratory Medicine, Kaohsiung Medical University Hospital, Kaohsiung 807, Taiwan*

Complete contact information is available at:
https://pubs.acs.org/10.1021/acsomega.3c02699

Author Contributions

[&]M.S. and C.-W.F. contributed equally to this work. M.S.: Data curation, formal analysis, project administration, writing—original draft; C.-W.F.: data curation, funding acquisition; I.-H.C.: data curation; A.K.: data curation; Y.C.W.: data curation; I.-L.L.: data curation; M.-J.T.: conceptualization and methodology; P.-C.W.: funding acquisition, investigation, writing, conceptualization, methodology, supervision, and review & editing. All authors have read and agreed to the published version of the manuscript

Notes

The authors declare no competing financial interest.

■ ACKNOWLEDGMENTS

■ REFERENCES

(1) Mersal, G. A. Experimental and computational studies on the electrochemical oxidation of caffeine at pseudo carbon paste electrode and its voltammetric determination in different real samples. *Food Anal. Methods* **2012**, *5*, 520−529.

(2) Buerge, I. J.; Poiger, T.; Müller, M. D.; Buser, H.-R. Caffeine, an anthropogenic marker for wastewater contamination of surface waters. *Environ. Sci. Technol.* **2003**, *37*, 691−700.

(3) Rigueto, C. V. T.; Nazari, M. T.; De Souza, C. F.; Cadore, J. S.; Brião, V. B.; Piccin, J. S. Alternative techniques for caffeine removal from wastewater: an overview of opportunities and challenges. *J. Water Process Eng.* **2020**, *35*, No. 101231.

(4) Alsabri, S. G.; Mari, W. O.; Younes, S.; Alsadawi, M. A.; Oroszi, T. L. Kinetic and Dynamic Description of Caffeine. *J. Caffeine Adenosine Res.* **2021**, *11*, 3.

(5) Blanchard, J.; Sawers, S. J. A. The absolute bioavailability of caffeine in man. *Eur. J. Clin. Pharmacol.* **1983**, *24*, 93−98.

(6) Teixeira, A. Z. A. Hydroxypropylcellulose controlled release tablet matrix prepared by wet granulation: effect of powder properties

and polymer composition. *Braz. Arch. Biol. Technol.* **2009**, *52*, 157−162.

(7) Amiri, M.; Salavati-Niasari, M.; Pardakhty, A.; Ahmadi, M.; Akbari, A. Caffeine: A novel green precursor for synthesis of magnetic CoFe(2)O(4) nanoparticles and pH-sensitive magnetic alginate beads for drug delivery. *Mater. Sci. Eng., C* **2017**, *76*, 1085−1093.

(8) Quintanilla de Stéfano, J. C.; Abundis-Correa, V.; Herrera-Flores, S. D.; Alvarez, A. J. pH-Sensitive Starch-Based Hydrogels: Synthesis and Effect of Molecular Components on Drug Release Behavior. *Polymers* **2020**, *12*, 1974.

(9) Alam, M. A.; Takafuji, M.; Ihara, H. Silica nanoparticle-crosslinked thermosensitive hybrid hydrogels as potential drug-release carriers. *Polym. J.* **2014**, *46*, 293−300.

(10) Cooley, M.; Sarode, A.; Hoore, M.; Fedosov, D. A.; Mitragotri, S.; Gupta, A. S. Influence of particle size and shape on their margination and wall-adhesion: implications in drug delivery vehicle design across nano-to-micro scale. *Nanoscale* **2018**, *10*, 15350−15364.

(11) Lv, H.; Xu, D.; Sun, L.; Henzie, J.; Suib, S. L.; Yamauchi, Y.; Liu, B. Ternary palladium−boron−phosphorus alloy mesoporous nanospheres for highly efficient electrocatalysis. *ACS Nano* **2019**, *13*, 12052−12061.

(12) Ban, C.; Jo, M.; Park, Y. H.; Kim, J. H.; Han, J. Y.; Lee, K. W.; Kweon, D.-H.; Choi, Y. J. Enhancing the oral bioavailability of curcumin using solid lipid nanoparticles. *Food Chem.* **2020**, *302*, No. 125328.

(13) Li, M.; Du, C.; Guo, N.; Teng, Y.; Meng, X.; Sun, H.; Li, S.; Yu, P.; Galons, H. Composition design and medical application of liposomes. *Eur. J. Med. Chem.* **2019**, *164*, 640−653.

(14) Li, A.; Zhao, J.; Fu, J.; Cai, J.; Zhang, P. Recent advances of biomimetic nano-systems in the diagnosis and treatment of tumor. *Asian J. Pharm. Sci.* **2021**, *16*, 161−174.

(15) Hajebi, S.; Rabiee, N.; Bagherzadeh, M.; Ahmadi, S.; Rabiee, M.; Roghani-Mamaqani, H.; Tahriri, M.; Tayebi, L.; Hamblin, M. R. Stimulus-responsive polymeric nanogels as smart drug delivery systems. *Acta Biomater.* **2019**, *92*, 1−18.

(16) Suhail, M.; Rosenholm, J. M.; Minhas, M. U.; Badshah, S. F.; Naeem, A.; Khan, K. U.; Fahad, M. Nanogels as drug-delivery systems: A comprehensive overview. *Ther. Delivery* **2019**, *10*, 697−717.

(17) Soni, G.; Yadav, K. S. Nanogels as potential nanomedicine carrier for treatment of cancer: A mini review of the state of the art. *Saudi Pharm. J.* **2016**, *24*, 133−139.

(18) Soni, K. S.; Desale, S. S.; Bronich, T. K. Nanogels: An overview of properties, biomedical applications and obstacles to clinical translation. *J. Controlled Release* **2016**, *240*, 109−126.

(19) Diouf, S. I. Y.; Williams, D. J.; Seifert, S.; Londoño-Calderon, A.; Pettes, M. T.; Sheehan, C. J.; Firestone, M. A. Multi-stimuli responsive tetra-PPO 60-PEO 20 ethylene diamine block copolymer enables pH, temperature, and solvent regulation of Au nanoparticle composite plasmonic response. *Polym. Chem.* **2019**, *10*, 6456−6472.

(20) Mackiewicz, M.; Romanski, J.; Krug, P.; Mazur, M.; Stojek, Z.; Karbarz, M. Tunable environmental sensitivity and degradability of nanogels based on derivatives of cystine and poly (ethylene glycols) of various length for biocompatible drug carrier. *Eur. Polym. J.* **2019**, *118*, 606−613.

(21) Yallapu, M. M.; Reddy, M. K.; Labhasetwar, V. Nanogels: chemistry to drug delivery. *Biomed. Appl. Nanotechnol.* **2007**, 131−171.

(22) Farazi, S.; Chen, F.; Foster, H.; Boquiren, R.; McAlpine, S. R.; Chapman, R. Real time monitoring of peptide delivery in vitro using high payload pH responsive nanogels. *Polym. Chem.* **2020**, *11*, 425−432.

(23) Azadi, A.; Hamidi, M.; Khoshayand, M.-R.; Amini, M.; Rouini, M.-R. Preparation and optimization of surface-treated methotrexate-loaded nanogels intended for brain delivery. *Carbohydr. Polym.* **2012**, *90*, 462−471.

(24) Shah, S.; Rangaraj, N.; Laxmikeshav, K.; Sampathi, S. Nanogels as drug carriers−Introduction, chemical aspects, release mechanisms and potential applications. *Int. J. Pharm.* **2020**, *581*, No. 119268.

(25) Urtuvia, V.; Maturana, N.; Acevedo, F.; Peña, C.; Díaz-Barrera, A. Bacterial alginate production: an overview of its biosynthesis and potential industrial production. *World J. Microbiol. Biotechnol.* **2017**, *33*, 1−10.

(26) Abasalizadeh, F.; Moghaddam, S. V.; Alizadeh, E.; Kashani, E.; Fazljou, S. M. B.; Torbati, M.; Akbarzadeh, A. Alginate-based hydrogels as drug delivery vehicles in cancer treatment and their applications in wound dressing and 3D bioprinting. *J. Biol. Eng.* **2020**, *14*, 1−22.

(27) Frachini, E. C. G.; Selva, J. S. G.; Falcoswki, P. C.; Silva, J. B.; Cornejo, D. R.; Bertotti, M.; Ulrich, H.; Petri, D. F. S. Caffeine Release from Magneto-Responsive Hydrogels Controlled by External Magnetic Field and Calcium Ions and Its Effect on the Viability of Neuronal Cells. *Polymers* **2023**, *15*, 1757.

(28) Amiryousefi, M. R.; Mohebbi, M.; Golmohammadzadeh, S.; Koocheki, A. Encapsulation of caffeine in hydrogel colloidosome: optimization of fabrication, characterization and release kinetics evaluation. *Flavour Fragrance J.* **2016**, *31*, 163−172.

(29) Nikoo, A. M.; Kadkhodaee, R.; Ghorani, B.; Razzaq, H.; Tucker, N. Electrospray-assisted encapsulation of caffeine in alginate microhydrogels. *Int. J. Biol. Macromol.* **2018**, *116*, 208−216.

(30) Belščak-Cvitanović, A.; Komes, D.; Karlović, S.; Djaković, S.; Špoljarić, I.; Mršić, G.; Ježek, D. Improving the controlled delivery formulations of caffeine in alginate hydrogel beads combined with pectin, carrageenan, chitosan and psyllium. *Food Chem.* **2015**, *167*, 378−386.

(31) Singha, N. R.; Dutta, A.; Mahapatra, M.; Roy, J. S. D.; Mitra, M.; Deb, M.; Chattopadhyay, P. K. In Situ Attachment of Acrylamido Sulfonic Acid-Based Monomer in Terpolymer Hydrogel Optimized by Response Surface Methodology for Individual and/or Simultaneous Removal(s) of M(III) and Cationic Dyes. *ACS Omega* **2019**, *4*, 1763−1780.

(32) Malik, N. S.; Ahmad, M.; Minhas, M. U.; Tulain, R.; Barkat, K.; Khalid, I.; Khalid, Q. Chitosan/Xanthan Gum Based Hydrogels as Potential Carrier for an Antiviral Drug: Fabrication, Characterization, and Safety Evaluation. *Front. Chem.* **2020**, 8.

(33) Abid, U.; Pervaiz, F.; Shoukat, H.; Rehman, S.; Abid, S. Fabrication and characterization of novel semi-IPN hydrogels based on xanthan gum and polyvinyl pyrrolidone-co-poly (2-acrylamido-2-methyl propane sulfonic acid) for the controlled delivery of venlafaxine. *Polym.-Plast. Technol. Mater.* **2022**, 577−592.

(34) Su, E.; Okay, O. Hybrid cross-linked poly(2-acrylamido-2-methyl-1-propanesulfonic acid) hydrogels with tunable viscoelastic, mechanical and self-healing properties. *React. Funct. Polym.* **2018**, *123*, 70−79.

(35) Dutta, A.; Mahapatra, M.; Deb, M.; Mitra, M.; Dutta, S.; Chattopadhyay, P. K.; Banerjee, S.; Sil, P. C.; Maiti, D. K.; Singha, N. R. Fluorescent Terpolymers Using Two Non-Emissive Monomers for Cr(III) Sensors, Removal, and Bio-Imaging. *ACS Biomater. Sci. Eng.* **2020**, *6*, 1397−1407.

(36) Mondal, H.; Karmakar, M.; Chattopadhyay, P. K.; Singha, N. R. Starch-g-tetrapolymer hydrogel via in situ attached monomers for removals of Bi(III) and/or Hg(II) and dye(s): RSM-based optimization. *Carbohydr. Polym.* **2019**, *213*, 428−440.

(37) Suhail, M.; Shih, C.-M.; Liu, J.-Y.; Hsieh, W.-C.; Lin, Y.-W.; Wu, P.-C. In-vitro and in-vivo evaluation of biocompatible polymeric microgels for pH-driven delivery of Ketorolac tromethamine. *Int. J. Pharm.* **2022**, *626*, No. 122194.

(38) Liu, W. Y.; Lin, C. C.; Hsieh, Y. S.; Wu, Y. T. Nanoformulation Development to Improve the Biopharmaceutical Properties of Fisetin Using Design of Experiment Approach. *Molecules* **2021**, *26*, 3031.

(39) Suhail, M.; Khan, A.; Rosenholm, J. M.; Minhas, M. U.; Wu, P. C. Fabrication and Characterization of Diclofenac Sodium Loaded Hydrogels of Sodium Alginate as Sustained Release Carrier. *Gels* **2021**, *7*, 10.

(40) Ullah, K.; Khan, S. A.; Murtaza, G.; Sohail, M.; Manan, A.; Afzal, A. Gelatin-based hydrogels as potential biomaterials for colonic delivery of oxaliplatin. *Int. J. Pharm.* **2019**, *556*, 236−245.

(41) Suhail, M.; Wu, P. C.; Minhas, M. U. Using Carbomer-Based Hydrogels for Control the Release Rate of Diclofenac Sodium: Preparation and In Vitro Evaluation. *Pharmaceuticals* **2020**, *13*, 399.

(42) Badshah, S. F.; Akhtar, N.; Minhas, M. U.; Khan, K. U.; Khan, S.; Abdullah, O.; Naeem, A. Porous and highly responsive cross-linked β-cyclodextrin based nanomatrices for improvement in drug dissolution and absorption. *Life Sci.* **2021**, *267*, No. 118931.

(43) Suhail, M.; Wu, P. C.; Minhas, M. U. Development and characterization of pH-sensitive chondroitin sulfate-co-poly(acrylic acid) hydrogels for controlled release of diclofenac sodium. *J. Saudi Chem. Soc.* **2021**, *25*, No. 101212.

(44) Khan, S.; Ranjha, N. M. Effect of degree of cross-linking on swelling and on drug release of low viscous chitosan/poly (vinyl alcohol) hydrogels. *Polym. Bull.* **2014**, *71*, 2133−2158.

(45) Öztürk, A. A.; Yenilmez, E.; Şenel, B.; Kıyan, H. T.; Güven, U. M. Effect of different molecular weight PLGA on flurbiprofen nanoparticles: formulation, characterization, cytotoxicity, and in vivo anti-inflammatory effect by using HET-CAM assay. *Drug Dev. Ind. Pharm.* **2020**, *46*, 682−695.

(46) Gonzalez-Pizarro, R.; Carvajal-Vidal, P.; Bellowa, L. H.; Calpena, A. C.; Espina, M.; García, M. L. In-situ forming gels containing fluorometholone-loaded polymeric nanoparticles for ocular inflammatory conditions. *Colloids Surf., B* **2019**, *175*, 365−374.

(47) Khan, K. U.; Minhas, M. U.; Sohail, M.; Badshah, S. F.; Abdullah, O.; Khan, S.; Munir, A.; Suhail, M. Synthesis of PEG-4000-co-poly (AMPS) nanogels by cross-linking polymerization as highly responsive networks for enhancement in meloxicam solubility. *Drug Dev. Ind. Pharm.* **2021**, *47*, 465−476.

(48) Peppas, N. A.; Sahlin, J. J. A simple equation for the description of solute release. III. Coupling of diffusion and relaxation. *Int. J. Pharm.* **1989**, *57*, 169−172.

(49) Sivagnanavelmurugan, M.; Radhakrishnan, S.; Palavesam, A.; Arul, V.; Immanuel, G. Characterization of alginic acid extracted from Sargassum wightii and determination of its anti-viral activity of shrimp Penaeus monodon post larvae against white spot syndrome virus. *Int. J. Curr. Res. Life Sci.* **2018**, *7*, 1863−1872.

(50) Shoukat, H.; Pervaiz, F.; Khan, M.; Rehman, S.; Akram, F.; Abid, U.; Noreen, S.; Nadeem, M.; Qaiser, R.; Ahmad, R.; Farooq, I. Development of β-cyclodextrin/polyvinypyrrolidone-co-poly (2-acryl-amide-2-methylpropane sulphonic acid) hybrid nanogels as nano-drug delivery carriers to enhance the solubility of Rosuvastatin: An in vitro and in vivo evaluation. *PLoS One* **2022**, *17*, No. e0263026.

(51) Rajam, K.; Rajendran, S.; Banu, N. N. Effect of caffeine-Zn2+ system in preventing corrosion of carbon steel in well water. *J. Chem.* **2013**, *2013*, 521951.

(52) Butt, S.; Hasan, S. M. F.; Hassan, M. M.; Alkharfy, K. M.; Neau, S. H. Directly compressed rosuvastatin calcium tablets that offer hydrotropic and micellar solubilization for improved dissolution rate and extent of drug release. *Saudi Pharm. J.* **2019**, *27*, 619−628.

(53) Khalid, I.; Ahmad, M.; Minhas, M. U.; Barkat, K.; Sohail, M. Cross-Linked Sodium Alginate-g-poly(Acrylic Acid) Structure: A Potential Hydrogel Network for Controlled Delivery of Loxoprofen Sodium. *Adv. Polym. Technol.* **2018**, *37*, 985−995.

(54) Sarmento, B.; Ferreira, D.; Veiga, F.; Ribeiro, A. Characterization of insulin-loaded alginate nanoparticles produced by ionotropic pre-gelation through DSC and FTIR studies. *Carbohydr. Polym.* **2006**, *66*, 1−7.

(55) Qiao, J.; Hamaya, T.; Okada, T. New highly proton-conducting membrane poly(vinylpyrrolidone)(PVP) modified poly(vinyl alcohol)/2-acrylamido-2-methyl-1-propanesulfonic acid (PVA-PAMPS) for low temperature direct methanol fuel cells (DMFCs). *Polymer* **2005**, *46*, 10809−10816.

(56) Barkat, K.; Ahmad, M.; Minhas, M. U.; Khalid, I. Oxaliplatin-loaded crosslinked polymeric network of chondroitin sulfate-co-poly (methacrylic acid) for colorectal cancer: Its toxicological evaluation. *J. Appl. Polym. Sci.* **2017**, *134*, 45312.

(57) Ali, L.; Ahmad, M.; Usman, M.; Yousuf, M. Controlled release of highly water-soluble antidepressant from hybrid copolymer poly vinyl alcohol hydrogels. *Polym. Bull.* **2014**, *71*, 31−46.

(58) Park, W.; Kim, K. S.; Bae, B. C.; Kim, Y. H.; Na, K. Cancer cell specific targeting of nanogels from acetylated hyaluronic acid with low molecular weight. *Eur. J. Pharm. Sci.* **2010**, *40*, 367−375.

(59) Hoare, T.; Young, S.; Lawlor, M. W.; Kohane, D. S. Thermoresponsive nanogels for prolonged duration local anesthesia. *Acta Biomater.* **2012**, *8*, 3596−3605.

(60) Fekete, T.; Borsa, J.; Takács, E.; Wojnárovits, L. Synthesis of cellulose-based superabsorbent hydrogels by high-energy irradiation in the presence of crosslinking agent. *Radiat. Phys. Chem.* **2016**, *118*, 114−119.

(61) Ranjha, N. M.; Ayub, G.; Naseem, S.; Ansari, M. T. Preparation and characterization of hybrid pH-sensitive hydrogels of chitosan-co-acrylic acid for controlled release of verapamil. *J. Mater. Sci.: Mater. Med.* **2010**, *21*, 2805−2816.

(62) Khalid, I.; Ahmad, M.; Minhas, M. U.; Barkat, K. Synthesis and evaluation of chondroitin sulfate based hydrogels of loxoprofen with adjustable properties as controlled release carriers. *Carbohydr. Polym.* **2018**, *181*, 1169−1179.

(63) Dergunov, S. A.; Nam, I. K.; Mun, G. A.; Nurkeeva, Z. S.; Shaikhutdinov, E. M. Radiation synthesis and characterization of stimuli-sensitive chitosan-polyvinyl pyrrolidone hydrogels. *Radiat. Phys. Chem.* **2005**, *72*, 619−623.

(64) Nasir, N.; Ahmad, M.; Minhas, M. U.; Barkat, K.; Khalid, M. F. pH-responsive smart gels of block copolymer [pluronic F127-co-poly (acrylic acid)] for controlled delivery of Ivabradine hydrochloride: Its toxicological evaluation. *J. Polym. Res.* **2019**, *26*, 1−15.

(65) Chen, S.-C.; Wu, Y.-C.; Mi, F.-L.; Lin, Y.-H.; Yu, L.-C.; Sung, H.-W. A novel pH-sensitive hydrogel composed of N, O-carboxymethyl chitosan and alginate cross-linked by genipin for protein drug delivery. *J. Controlled Release* **2004**, *96*, 285−300.

(66) Lim, S. L.; Tang, W. N. H.; Ooi, C. W.; Chan, E. S.; Tey, B. T. Rapid swelling and deswelling of semi-interpenetrating network poly(acrylic acid)/poly(aspartic acid) hydrogels prepared by freezing polymerization. *J. Appl. Polym. Sci.* **2016**, *133*, 43515.

(67) Şanlı, O.; Ay, N.; Işıklan, N. Release characteristics of diclofenac sodium from poly (vinyl alcohol)/sodium alginate and poly (vinyl alcohol)-grafted-poly (acrylamide)/sodium alginate blend beads. *Eur. J. Pharm. Biopharm.* **2007**, *65*, 204−214.

(68) Pourjavadi, A.; Hosseinzadeh, H.; Mazidi, R. Modified carrageenan. 4. Synthesis and swelling behavior of crosslinked κC-g-AMPS superabsorbent hydrogel with antisalt and pH-responsiveness properties. *J. Appl. Polym. Sci.* **2005**, *98*, 255−263.

(69) Khan, K. U.; Akhtar, N.; Minhas, M. U. Poloxamer-407-Co-Poly (2-Acrylamido-2-Methylpropane Sulfonic Acid) Cross-linked Nanogels for Solubility Enhancement of Olanzapine: Synthesis, Characterization, and Toxicity Evaluation. *AAPS PharmSciTech* **2020**, *21*, 141.

(70) Peng, G.; Xu, S.; Peng, Y.; Wang, J.; Zheng, L. A new amphoteric superabsorbent hydrogel based on sodium starch sulfate. *Bioresour. Technol.* **2008**, *99*, 444−447.

(71) Wu, W.; Wang, D. S. A fast pH-responsive IPN hydrogel: Synthesis and controlled drug delivery. *React. Funct. Polym.* **2010**, *70*, 684−691.

(72) Murthy, P. S. K.; Mohan, Y. M.; Sreeramulu, J.; Raju, K. M. Semi-IPNs of starch and poly(acrylamide-co-sodium methacrylate): Preparation, swelling and diffusion characteristics evaluation. *React. Funct. Polym.* **2006**, *66*, 1482−1493.

(73) Khanum, H.; Ullah, K.; Murtaza, G.; Khan, S. A. Fabrication and in vitro characterization of HPMC-g-poly(AMPS) hydrogels loaded with loxoprofen sodium. *Int. J. Biol. Macromol.* **2018**, *120*, 1624−1631.

(74) Kulkarni, R. V.; Sa, B. Polyacrylamide-grafted-alginate-based pH-sensitive hydrogel beads for delivery of ketoprofen to the intestine: in vitro and in vivo evaluation. *J. Biomater. Sci., Polym. Ed.* **2009**, *20*, 235−251.

(75) Al-Tabakha, M. M.; Khan, S. A.; Ashames, A.; Ullah, H.; Ullah, K.; Murtaza, G.; Hassan, N. Synthesis, Characterization and Safety Evaluation of Sericin-Based Hydrogels for Controlled Delivery of Acyclovir. *Pharmaceuticals* **2021**, *14*, 234.

(76) Siepmann, J.; Peppas, N. A. Modeling of drug release from delivery systems based on hydroxypropyl methylcellulose (HPMC). *Adv. Drug Delivery Rev.* **2012**, *64*, 163−174.

(77) Hsieh, W.-C.; Fang, C.-W.; Suhail, M.; Vu, Q. L.; Chuang, C.-H.; Wu, P.-C. Improved skin permeability and whitening effect of catechin-loaded transfersomes through topical delivery. *Int. J. Pharm.* **2021**, *607*, No. 121030.